

Spectroscopic and Thermodynamic Investigations of Transition-Metal Cluster Ions in the Gas Phase: Photodissociation of MFe^+

R. L. Hettich and B. S. Freiser*

Contribution from the Department of Chemistry, Purdue University, West Lafayette, Indiana 47907. Received June 11, 1986

Abstract: Heteronuclear metal dimer ions, MFe^+ ($M = Sc, Ti, V, Cr, Fe, Co, Ni, Cu, Nb, Ta$), were generated and isolated in the gas phase with use of Fourier transform mass spectrometry. Observation of these ionic species in a ligand-free environment provides a method of probing the fundamental bonding nature between two bare transition-metal atoms. The photodissociation spectra of MFe^+ , obtained by monitoring the fragmentation of MFe^+ as a function of wavelength, provide both spectroscopic and thermodynamic information. Both M^+ and Fe^+ are observed as photoproducts, with the metal having the lowest ionization potential predominating. The photodissociation spectra reveal broad absorption in the ultraviolet and visible spectral regions with a range of cross sections from 0.06 \AA^2 for VFe^+ to 0.62 \AA^2 for $CrFe^+$. Bond energies obtained by observing photoappearance onsets are in the range of 48 kcal/mol for $ScFe^+$ to 75 kcal/mol for VFe^+ and show good agreement with values obtained by ion-molecule bracketing techniques, suggesting that the observed thresholds are thermodynamic and not spectroscopic. The metal cluster ions are found in general to be bound more strongly than their neutral metal dimer counterparts. The ionization potentials for MFe can be calculated from $D^0(M-Fe)$ and $D^0(M^+-Fe)$ and are found to be in the range of 5.4 eV for VFe to 7.4 eV for $TaFe$.

Examination of the bonding and energetics of small bare metal clusters has become a topic of considerable interest in recent years.¹⁻⁴ Bare metal clusters are thought to mimic metal surfaces, and investigating their reactivity may help probe the nature of catalytic activity. Extensive theoretical calculations have been performed for a variety of neutral transition-metal dimers, but the difficulty in determining the ground electronic state makes the results somewhat ambiguous.³ The intense theoretical activity in this area is directed at understanding how important the d electrons are to the bonding in these metal clusters.

Previous investigations of bare transition-metal clusters have utilized rare gas matrix isolation techniques and gas phase techniques including multiphoton ionization and laser-induced fluorescence. Knudsen cell mass spectrometry has been used to obtain bond energies for most homonuclear transition-metal dimers.⁵ Recent instrumental developments have made possible the generation of many different types and sizes of clusters. These new methods include sputtering techniques,⁶ gas evaporation techniques,⁷ supersonic expansion techniques with oven⁸ and pulsed laser sources,⁹ and multiphoton dissociation of metal cluster organometallics.¹⁰ Recently, our laboratory demonstrated the synthesis of homonuclear and heteronuclear transition-metal cluster ions using Fourier transform mass spectrometry.¹¹ This method utilizes an ion-molecule reaction between a metal ion and an appropriate metal carbonyl neutral, followed by collision-in-

duced dissociation to strip off the remaining carbonyls, resulting in the generation of the selected cluster ion. Homonuclear and heteronuclear dimer and trimer ions have been made by this route.

Photodissociation has been utilized to obtain spectral information about gas-phase ions, especially organic ions.¹² Recently, photodissociation studies on inorganic ions have suggested that, in many cases, both spectroscopic and thermodynamic information can be obtained.¹³⁻¹⁵ The photodissociation spectrum of VFe^+ revealed two absorption maxima at 260 and 340 nm as well as a dissociation threshold at 380 nm, implying $D^0(V^+-Fe) = 75 \pm 5$ kcal/mol, which was in good agreement with a bond energy determined by ion-molecule bracketing.¹⁶ Bowers et al. have recently reported the photodissociation of Mn_2^+ using a crossed ion beam-laser apparatus and obtained $D^0(Mn^+-Mn) \geq 1.39$ eV by observing kinetic energy distributions of the photofragments.¹⁷ This value is higher than $D^0(Mn^+-Mn) = 0.85 \pm 0.2$ eV previously reported.¹⁸

In this paper we extend our studies of VFe^+ by examining the photodissociation of MFe^+ , where M is an element of the 3d transition-metal series. Photoappearance thresholds should give values for both $D^0(M^+-Fe)$ and $D^0(Fe^+-M)$ directly. Alternatively, once $D^0(M^+-Fe)$ is known, $D^0(Fe^+-M)$ can be calculated by using the difference in ionization potentials of M and Fe . $MnFe^+$ was not generated due to the difficulty of obtaining a suitable manganese target for producing Mn^+ . In addition to VFe^+ , $NbFe^+$ and $TaFe^+$ were examined to probe changes that occur in a given column of the Periodic Table. Photodissociation provides information about photoproducts, spectral band positions, cross sections for dissociation, and photoappearance thresholds. References to the bonding of neutral metal clusters will be cited in the appropriate sections for comparison to the ionic clusters.

Experimental Section

The theory, instrumentation, and methodology of Fourier transform mass spectrometry (FTMS) have been described elsewhere.¹⁹ All ex-

- (1) Miedema, A. R. *Faraday Symp. Chem. Soc.* **1980**, *14*, 136.
- (2) Gingerich, K. A. *Faraday Symp. Chem. Soc.* **1980**, *14*, 109.
- (3) Weltner, W., Jr.; Van Zee, R. *J. Annu. Rev. Phys. Chem.* **1984**, *35*, 291.
- (4) Klyagina, A. P.; Levin, A. A. *Koord. Khim.* **1984**, *10*, 317.
- (5) (a) Gupta, S. K.; Nappi, B. M.; Gingerich, K. A. *Inorg. Chem.* **1981**, *20*, 966. (b) Gingerich, K. A. *J. Cryst. Growth* **1971**, *9*, 31.
- (6) (a) Winograd, N.; Harrison, D. E., Jr.; Garrison, B. J. *Surf. Sci.* **1978**, *78*, 467. (b) Freas, R. B.; Campana, J. E. *J. Am. Chem. Soc.* **1985**, *107*, 6202. (c) Hanley, L.; Anderson, S. L. *Chem. Phys. Lett.* **1986**, *129*, 429.
- (7) (a) Sattler, K.; Muhlbach, J.; Recknagel, E. *Phys. Rev. Lett.* **1980**, *45*, 821. (b) Abe, H.; Schulze, W.; Tesche, B. *Chem. Phys.* **1980**, *47*, 95.
- (8) (a) Riley, S. J.; Parks, E. K.; Mao, C. R.; Poppo, L. G.; Wexler, S. J. *Phys. Chem.* **1982**, *86*, 3911. (b) Gole, J. L.; Green, G. J.; Pace, S. H.; Preuss, D. R. *J. Chem. Phys.* **1982**, *76*, 2247.
- (9) (a) Bondybey, V. E.; English, J. H. *J. Chem. Phys.* **1982**, *74*, 6978. (b) Morse, M. D.; Smalley, R. E. *Ber. Bunsenges Phys. Chem.* **1984**, *88*, 228. (c) Morse, M. D.; Hansen, G. P.; Langridge-Smith, P. R. R.; Zheng, L.-S.; Geusic, M. E.; Michalopoulos, D. L.; Smalley, R. E. *J. Chem. Phys.* **1984**, *80*, 5400.
- (10) Leopold, D. G.; Vaida, V. *J. Am. Chem. Soc.* **1983**, *105*, 6809.
- (11) (a) Jacobson, D. B.; Freiser, B. S. *J. Am. Chem. Soc.* **1985**, *107*, 1581. (b) Jacobson, D. B.; Freiser, B. S. *J. Am. Chem. Soc.* **1984**, *106*, 5351.

- (12) Dunbar, R. C. *Gas Phase Ion Chemistry*, Bowers, M. T., Ed.; Academic Press: New York, 1984; Vol. 3, Chapter 20.
- (13) Hettich, R. L.; Freiser, B. S. *J. Am. Chem. Soc.* **1986**, *108*, 2357.
- (14) Cassidy, C. J.; Freiser, B. S. *J. Am. Chem. Soc.* **1984**, *106*, 6176.
- (15) Hettich, R. L.; Jackson, T. C.; Stanko, E. M.; Freiser, B. S. *J. Am. Chem. Soc.* **1986**, *108*, 5086.
- (16) Hettich, R. L.; Freiser, B. S. *J. Am. Chem. Soc.* **1985**, *107*, 6222.
- (17) Jarrold, M. F.; Illies, A. J.; Bowers, M. T. *J. Am. Chem. Soc.* **1985**, *107*, 7339.
- (18) Ervin, K.; Loh, S. K.; Aristov, N.; Armentrout, P. B. *J. Phys. Chem.* **1983**, *87*, 3593.
- (19) (a) Comisarow, M. B.; Marshall, A. G. *Chem. Phys. Lett.* **1974**, *26*, 489. (b) Comisarow, M. B. *Adv. Mass Spectrom.* **1980**, *8*, 1698.

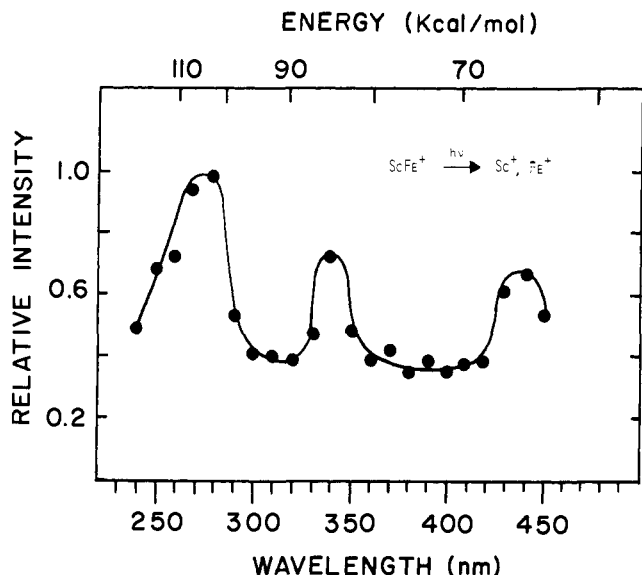


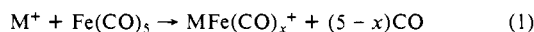
Figure 1. The photodissociation spectrum of ScFe^+ obtained by monitoring the appearance of Sc^+ and Fe^+ as a function of wavelength.

periments were performed on a Nicolet prototype FTMS-1000 Fourier transform mass spectrometer²⁰ equipped with a 5.2 cm cubic trapping cell situated between the poles of a Varian 15-in. electromagnet maintained at 0.90 T. The cell, which is contained in a vacuum chamber maintained at a background pressure of $\sim 1 \times 10^{-8}$ Torr, was constructed in our laboratory and in this study utilized two 80% transmittance stainless steel screens as the transmitter plates. This configuration permitted irradiation with a 2.5-kW Hg-Xe arc lamp, used in conjunction with a Schoeffel 0.25-m monochromator set for 10-nm resolution. Metal ions were generated by focusing the frequency doubled beam (532 nm) of a Quanta Ray Nd:YAG laser into the center-drilled hole (1 mm) of a high-purity rod of the appropriate metal supported on the transmitter screen nearest to the laser.²¹

All chemicals used in this study were obtained commercially and used without further purification, except for multiple freeze-pump-thaw cycles to remove noncondensable gases. $\text{Fe}(\text{CO})_5$ was introduced into the vacuum chamber through a General Valve Corp. Series 9 pulsed solenoid valve.²² Use of the pulsed valve allows the ion of interest to be trapped in the absence of competing ion-molecule reactions with the neutral iron pentacarbonyl. All other reagent gases were admitted to the cell through variable leak valves.

Details of the collision-induced dissociation (CID) experiment have been given elsewhere.²³ Argon was used as the collision gas at a total static pressure of $\sim 1 \times 10^{-5}$ Torr. The translational energy of the ions can be varied and is typically in the range of 0–100 eV. A Bayard-Alpert ionization gauge was used to monitor the static pressures.

The metal cluster ions (MFe^+) were generated by a two-step procedure which was initially outlined for CoFe^+ .¹¹ Laser desorbed metal ions, M^+ where $\text{M} = \text{Sc}, \text{Ti}, \text{V}, \text{Cr}, \text{Fe}, \text{Co}, \text{Ni}, \text{Cu}, \text{Nb}, \text{and Ta}$, react with $\text{Fe}(\text{CO})_5$ to displace one or more carbonyls (reaction 1). The major metal cluster carbonyl ion is isolated with swept double resonance pulses



and then accelerated to ~ 50 – 100 eV kinetic energy. Inelastic collisions with the argon target gas result in sequential loss of carbonyls to produce MFe^+ . Once generated, the bare metal cluster ions were trapped for 3–6 s, depending on the cross section for photodissociation, either in the presence or absence of radiation from the arc lamp. The relatively high static pressure of argon is believed to allow the excess energy of the clusters to be dissipated by thermalizing collisions. However, the presence of some internal energy, which would yield bond energies which are too low, cannot be completely ruled out.

Photodissociation spectra were obtained by monitoring the appearance of ionic photoproducts as a function of the wavelength of light.²⁴ Each

(20) Cody, R. B.; Burnier, R. C.; Freiser, B. S. *Anal. Chem.* **1982**, *54*, 96.

(21) Burnier, R. C.; Byrd, G. D.; Freiser, B. S. *J. Am. Chem. Soc.* **1981**, *103*, 4360.

(22) For a description of pulsed valve operation, see: Carlin, T. J.; Freiser, B. S. *Anal. Chem.* **1983**, *55*, 571.

(23) Burnier, R. C.; Cody, R. B.; Freiser, B. S. *J. Am. Chem. Soc.* **1982**, *104*, 7436.

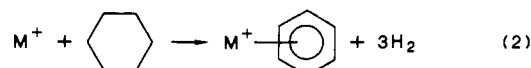
Table I. Thermodynamic Data for Metal Clusters

AB	$D^\circ(\text{A-B})^a$ (kcal/mol)	$\text{IP}(\text{AB})^b$ (eV)	$D^\circ(\text{A}^+-\text{B})$ (kcal/mol)	$D^\circ(\text{A}^+-\text{B})$ (kcal/mol)	$D^\circ(\text{B}^+-\text{A})$ (kcal/mol)
ScFe	55	6.8	48 ± 5	49 ± 6^d	79 ± 5
TiFe	42	6.0	60 ± 6	>49	84 ± 6
VFe	44	5.4	75 ± 5^e	$>62^f$	101 ± 5
CrFe	32	6.0	50 ± 7	g	75 ± 7
Fe_2	18	6.0	62 ± 5	58 ± 7^h	62 ± 5
CoFe	30	6.5	62 ± 5	62 ± 6^h	62 ± 5
NiFe	39	6.6	64 ± 5	$<68 \pm 5^i$	69 ± 5
CuFe	30	6.7	53 ± 7	>52	56 ± 7
NbFe	59^j	6.5	68 ± 5	$>60^k$	91 ± 5
TaFe	60^j	7.4	72 ± 5	$>60^k$	72 ± 5

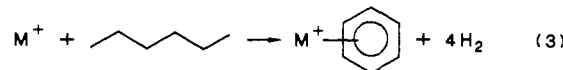
^aTheoretical values obtained from ref 3. Value for Fe_2 also obtained experimentally, ref 40. ^bDerived from theoretical $D^\circ(\text{A-B})$ and experimental $D^\circ(\text{A}^+-\text{B})$. ^cCalculated from $D^\circ(\text{A}^+-\text{B})$ with $\text{IP}(\text{A})$ and $\text{IP}(\text{B})$. ^dReference 28. ^eReference 16. ^fReference 15. ^gIndeterminate, see text. ^hReference 33. ⁱReference 37. ^jReference 1. ^kReference 39. ^lPDS = photodissociation. ^m1-M = ion-molecule reactions.

photodissociation spectrum is the result of several trials, indicating reproducibilities for peak heights of $\pm 40\%$ and peak positions of ± 10 nm. Photodissociation thresholds were determined with white light and cutoff filters and, whenever light intensity permitted (i.e., for $\lambda < 450$ nm), confirmed with the monochromator. To obtain absolute values for the cross sections of the ions being examined, the photodissociation of C_7H_8^+ (from toluene at 20 eV) at 410 nm ($\sigma = 0.05 \text{ \AA}^2$)²⁵ was compared to the photodissociation of a given ion at its λ_{max} , both taken under similar experimental conditions. All cross sections determined in this manner have an estimated uncertainty of $\pm 50\%$ due to instrumental variables.

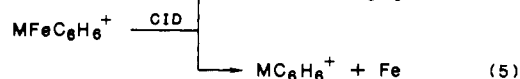
In order for us to check the thermodynamic values of MFe^+ determined by photodissociation thresholds, ion-molecule reactions and collision-induced dissociation were used to bracket the bond energies of MFe^+ . The observation of a given reaction in the gas phase implies a lower limit for the enthalpy of that reaction.²⁶ For example, if reaction 2 is observed, then $D^\circ(\text{M}^+-\text{C}_6\text{H}_6) > 49$ kcal/mol is estimated, which is



the energy required to dehydrogenate cyclohexane to benzene.²⁷ If reaction 3 is observed, then $D^\circ(\text{M}^+-\text{C}_6\text{H}_6) > 60$ kcal/mol. The absence



of a given reaction does not necessarily imply an upper limit for reaction enthalpy since other complicating factors (e.g., kinetics, electronic nature) may be controlling. Once $D^\circ(\text{M}^+-\text{C}_6\text{H}_6)$ is known (or at least defined by a lower limit), it can be used to bracket $D^\circ(\text{M}^+-\text{Fe})$. $\text{MFeC}_6\text{H}_6^+$ can be made by reacting MFe^+ with cyclohexene. Collision-induced dissociation of $\text{MFeC}_6\text{H}_6^+$ (along with observing the reaction between MFe^+ and benzene) will indicate which dissociation channel, reaction 4 or 5, is lower in energy. If reaction 4 is observed, then $D^\circ(\text{M}^+-\text{Fe}) >$



$D^\circ(\text{M}^+-\text{C}_6\text{H}_6)$ is implied. If reaction 5 is observed, then $D^\circ(\text{M}^+-\text{C}_6\text{H}_6)$ provides an upper limit for the bond energy of MFe^+ . If both reactions 4 and 5 are observed, then $D^\circ(\text{M}^+-\text{Fe})$ is within ~ 1 – 3 kcal/mol of $D^\circ(\text{M}^+-\text{C}_6\text{H}_6)$.

Results and Discussion

(MFe)⁺ Photodissociation. ScFe^+ . ScFe^+ photodissociates to give Sc^+ as the major photoproduct and Fe^+ . The photodisso-

(24) The low concentration of ions in the cell ($\sim 10^{-18}$ M) precludes monitoring the absorbance of the light directly.

(25) Dunbar, R. C. *Chem. Phys. Lett.* **1975**, *32*, 508.

(26) Observation of a gas-phase reaction (occurring with an appreciable rate) is assumed to imply exothermicity ($\Delta H^\circ_{\text{rxn}} < 0$). However, there is some uncertainty, possibly ± 5 kcal/mol, in the values used as lower limits.

(27) All heats of formation and ionization potentials are taken from the following: Rosenstock, H. M.; Draxl, K.; Steiner, B. W.; Herron, J. T. *J. Phys. Chem. Ref. Data, Suppl.* **1** 1977, 6.

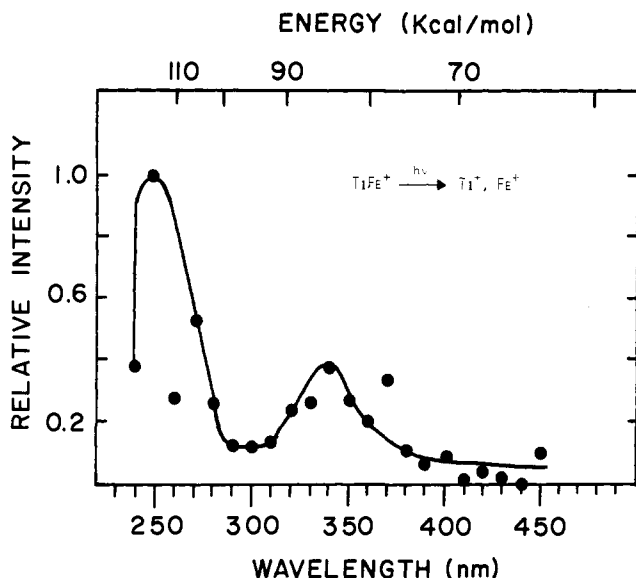
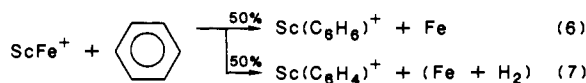


Figure 2. The photodissociation spectrum of $TiFe^+$ obtained by monitoring the appearance of Ti^+ and Fe^+ as a function of wavelength.

ciation spectrum, shown in Figure 1, reveals dissociation throughout the entire ultraviolet region, with peak maxima at 280 ($\sigma = 0.32 \text{ \AA}^2$), 340, and 440 nm. The photoappearance threshold for Sc^+ from $ScFe^+$ occurs at 600 nm, determined with cutoff filters, implying $D^\circ(Sc^+-Fe) = 48 \pm 5 \text{ kcal/mol}$. The threshold for photoappearance of Fe^+ , which was difficult to determine, occurs between 340 and 400 nm, implying $71 \text{ kcal/mol} < D^\circ(Fe^+-Sc) < 84 \text{ kcal/mol}$. When $D^\circ(Sc^+-Fe) = 48 \pm 5 \text{ kcal/mol}$ and the ionization potentials of Fe and Sc are used,²⁷ $D^\circ(Fe^+-Sc) = 79 \pm 5 \text{ kcal/mol}$ is obtained. Table I summarizes the bond energies for the metal cluster ions examined in this report.

$ScFe^+$ will react with benzene to fragment the cluster ion, reactions 6 and 7. CID of $ScFeC_6H_6^+$, obtained by reacting

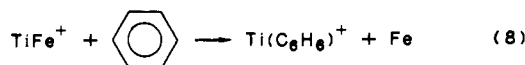


cyclohexene with $ScFe^+$, results in formation primarily of $ScC_6H_6^+$, with a small amount of $ScFe^+$ also observed. These results indicate that $D^\circ(Sc^+-Fe)$ is slightly less ($\sim 1\text{--}3 \text{ kcal/mol}$) than $D^\circ(Sc^+-C_6H_6) = 52 \pm 5 \text{ kcal/mol}$ ²⁸ and is assigned $D^\circ(Sc^+-Fe) = 49 \pm 6 \text{ kcal/mol}$. The formation of $ScC_6H_4^+$, which presumably is Sc^+ -benzyne, in reaction 7 may be facilitated by the formation of FeH_2 .²⁹

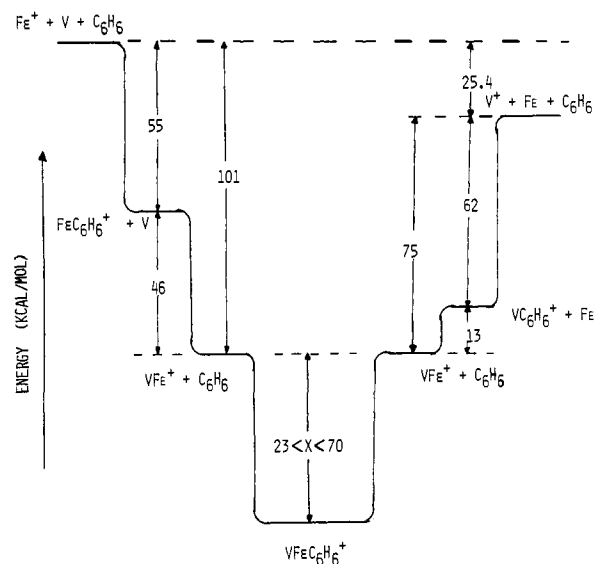
No experimental data for $ScFe$ have been obtained, but a theoretical value of $D^\circ(Sc-Fe) = 55 \text{ kcal/mol}$ has been predicted.³ Ionization of $ScFe$ weakens the metal-metal bond, suggesting that ionization removes a bonding electron.

TiFe⁺. The photodissociation spectrum of $TiFe^+$, shown in Figure 2, reveals two peaks at 250 ($\sigma = 0.22 \text{ \AA}^2$) and 340 nm. The threshold for photoappearance of Ti^+ , which is the major photoproduct, is difficult to determine due to a low cross section for dissociation in the visible region and is found to occur between 430 and 510 nm (these two wavelengths are intense spectral lines output from the arc lamp), implying $D^\circ(Ti^+-Fe) = 60 \pm 6 \text{ kcal/mol}$ and $D^\circ(Fe^+-Ti) = 84 \pm 6 \text{ kcal/mol}$. The threshold for appearance of Fe^+ occurs between 300 and 380 nm, suggesting $75 \text{ kcal/mol} < D^\circ(Fe^+-Ti) < 95 \text{ kcal/mol}$.

Benzene reacts slowly with $TiFe^+$ to displace Fe exclusively (reaction 8). $TiFeC_6H_6^+$, formed by reaction of $TiFe^+$ with



Scheme I. Energetics for the $[V-Fe-C_6H_6]^+$ System



cyclohexene, undergoes collision-induced dissociation to yield primarily $TiFe^+$ with a minor amount of $TiC_6H_6^+$ also observed. These results imply $D^\circ(Ti^+-Fe)$ is only slightly greater (ca. 1–3 kcal/mol) than $D^\circ(Ti^+-C_6H_6)$. Thus, reaction 8, which is endothermic by 1–3 kcal/mol, can be observed as a slow reaction.



Observation of reaction 9 provides a lower limit of $D^\circ(Ti^+-C_6H_6) > 49 \text{ kcal/mol}$, consistent with the above interpretation.

Theoretical examination has suggested that the ground state of $TiFe$ is $^1\Sigma$ (extensive d electron bonding) and $D^\circ(Ti-Fe) = 42 \text{ kcal/mol}$,³ although no experimental data have been obtained.

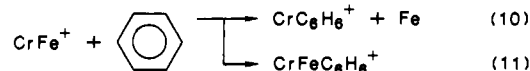
VFe⁺. Photodissociation of VFe^+ has recently been reported.¹⁶ Peak maxima in the photodissociation spectrum occur at 260 and 340 nm ($\sigma = 0.06 \text{ \AA}^2$), and a threshold was observed at 380 nm, implying $D^\circ(V^+-Fe) = 75 \pm 5 \text{ kcal/mol}$ and $D^\circ(Fe^+-V) = 101 \pm 5 \text{ kcal/mol}$. V^+ was observed as the only photoproduct, even at 240 nm, possibly due to the low cross section of VFe^+ for photodissociation in this region.

VFe^+ reacts with benzene to form a condensation complex exclusively. Collision-induced dissociation of the $VFe(C_6H_6)^+$ yields predominantly VFe^+ (benzene elimination) with some V^+ observed at high energy. These results yield lower limits of $D^\circ(Fe^+-V) > D^\circ(Fe^+-C_6H_6) = 55 \pm 5 \text{ kcal/mol}$ ¹⁵ and $D^\circ(V^+-Fe) > D^\circ(V^+-C_6H_6) = 62 \pm \text{kcal/mol}$,¹⁵ both consistent with the photodissociation results. Scheme I illustrates the energetics for the $[V-Fe-C_6H_6]^+$ system.²⁷

A low spin ground state, involving both s and d electron bonding, has been postulated for VFe with $D^\circ(V-Fe) = 44 \text{ kcal/mol}$.^{1,3}

CrFe⁺. $CrFe^+$ photodissociates readily in the ultraviolet region to produce both Cr^+ and Fe^+ as photoproducts. Peaks at 250 ($\sigma = 0.62 \text{ \AA}^2$) and 340 nm are observed in the photodissociation spectrum (Figure 3). An appearance threshold for Cr^+ is observed at 570 nm, implying $D^\circ(Cr^+-Fe) = 50 \pm 7 \text{ kcal/mol}$ and $D^\circ(Fe^+-Cr) = 75 \pm 7 \text{ kcal/mol}$. The photoappearance threshold for Fe^+ at 400 nm, implying $D^\circ(Fe^+-Cr) = 72 \pm 7 \text{ kcal/mol}$, is consistent with these values.

Benzene reacts with $CrFe^+$ to produce primarily $CrC_6H_6^+$, with a small amount of $CrFeC_6H_6^+$ also observed (reactions 10 and 11). Collision-induced dissociation of $CrFeC_6H_6^+$, formed by



reacting $CrFe^+$ with cyclohexene, produces predominantly $CrC_6H_6^+$ with some $CrFe^+$ also formed. These results indicate that $D^\circ(Cr^+-Fe)$ is slightly less than $D^\circ(Cr^+-C_6H_6)$, suggesting

(28) Lech, L. M.; Freiser, B. S., unpublished results.

(29) $\Delta H_f^\circ(FeH_2) < 77.5 \text{ kcal/mol}$: Halle, L. F.; Klein, F. S.; Beauchamp, J. L. J. Am. Chem. Soc. 1984, 106, 2543.

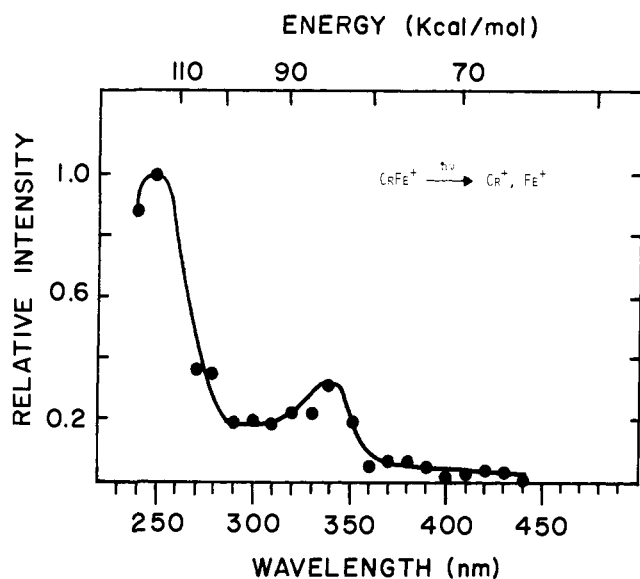


Figure 3. The photodissociation spectrum of CrFe^+ obtained by monitoring the appearance of Cr^+ and Fe^+ as a function of wavelength.

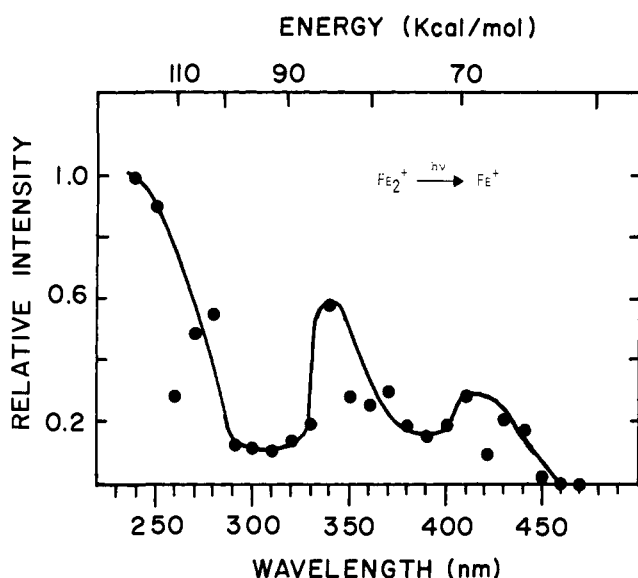


Figure 4. The photodissociation spectrum of Fe_2^+ obtained by monitoring the appearance of Fe^+ as a function of wavelength.

$D^\circ(\text{Cr}^+-\text{C}_6\text{H}_6) = 53 \pm 9$ kcal/mol. Cr^+ will dehydrogenate cyclohexene to benzene, implying $D^\circ(\text{Cr}^+-\text{C}_6\text{H}_6) > 21$ kcal/mol, but no reaction is observed between Cr^+ and cyclohexane, possibly indicating $D^\circ(\text{Cr}^+-\text{C}_6\text{H}_6) < 49$ kcal/mol. However, Cr^+ is unreactive with many alkanes and, thus, this upper limit is speculative.

Examination of CrFe in a rare gas matrix suggests that both s and d electrons are involved in bonding.³⁰ A theoretical value of $D^\circ(\text{Cr}-\text{Fe}) = 32$ kcal/mol has been calculated.³

Fe_2^+ . Figure 4, the photodissociation spectrum of Fe_2^+ , reveals three peaks at 240 ($\sigma = 0.27 \text{ \AA}^2$), 340, and 430 nm. The photoappearance of Fe^+ is observed out to 460 nm, suggesting $D^\circ(\text{Fe}^+-\text{Fe}) = 62 \pm 5$ kcal/mol. The visible absorption spectrum of Fe_2 in an argon matrix has been obtained and shows broad absorption in the 370–540 nm range with peak maxima at 380, 415, and 470 nm.^{31a} Interestingly, theoretical calculations of Fe_2 indicate 112 electronic states less than 0.5 eV above the ground state.³²

(30) Nagarathana, H. M.; Montano, P. A.; Naik, V. M. *J. Am. Chem. Soc.* **1983**, *105*, 2938.

(31) (a) DeVore, T. C.; Ewing, A.; Franzen, H. F.; Calder, V. *Chem. Phys. Lett.* **1975**, *35*, 78. (b) Moskovits, M.; Hulse, J. E. *J. Chem. Phys.* **1977**, *66*, 3988.

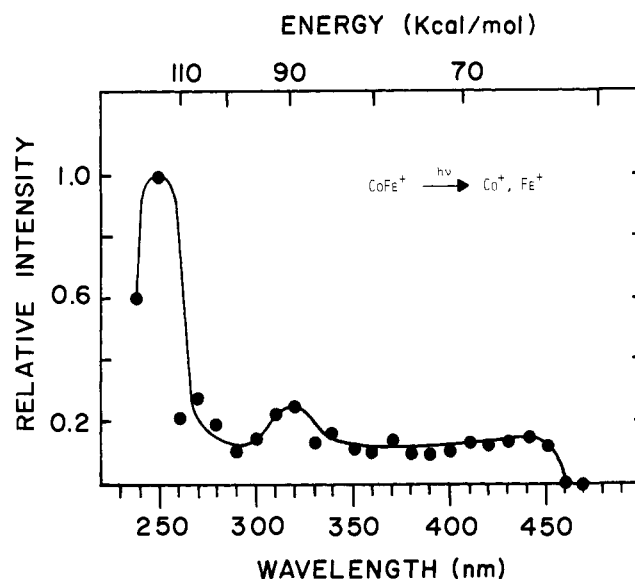


Figure 5. The photodissociation spectrum of CoFe^+ obtained by monitoring the appearance of Co^+ and Fe^+ as a function of wavelength.

Benzene reacts slowly with Fe_2^+ to yield FeC_6H_6^+ exclusively (reaction 12). In addition, collisional activation of $\text{Fe}_2\text{C}_6\text{H}_6^+$ yields

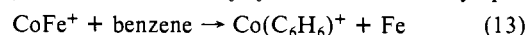


predominantly Fe_2^+ with some FeC_6H_6^+ also observed at high kinetic energy, suggesting $D^\circ(\text{Fe}^+-\text{Fe}) > D^\circ(\text{Fe}^+-\text{benzene}) = 55 \pm 5$ kcal/mol.¹⁵ These results imply $D^\circ(\text{Fe}^+-\text{Fe}) = 58 \pm 7$ kcal/mol, which is in reasonable agreement with the photodissociation result as well as a previously reported value of $D^\circ(\text{Fe}^+-\text{Fe}) = 64 \pm 7$ kcal/mol.³³ Finally, Smalley and co-workers have also measured the one-photon dissociation threshold of Fe_2^+ , suggesting a bond energy of the metal dimer ion between 56 and 67 kcal/mol.³⁴ The excellent agreement between this value and the photodissociation result of 62 kcal/mol is significant since the cluster ion generated in Smalley's supersonic expansion experiment was relaxed prior to photofragmentation.

The bonding in Fe_2 is thought to be due entirely to 4s orbital overlap with $D^\circ(\text{Fe}-\text{Fe}) = 18$ kcal/mol,³ although the presence of some d bonding has been postulated.^{30,35}

CoFe^+ . CoFe^+ photodissociates to give both Co^+ and Fe^+ in roughly a 2:1 ratio, respectively. Figure 5 illustrates the one major peak observed at 250 nm ($\sigma = 0.30 \text{ \AA}^2$) in the photodissociation spectrum of CoFe^+ . Dissociation thresholds for both Fe^+ and Co^+ are observed at 460 nm, implying $D^\circ(\text{Co}^+-\text{Fe}) \sim D^\circ(\text{Fe}^+-\text{Co}) = 62 \pm 5$ kcal/mol.

CoFe^+ reacts readily with benzene by displacing Fe exclusively (reaction 13). In addition $\text{CoFeC}_6\text{H}_6^+$ loses Fe exclusively upon



collisional activation. These results yield $D^\circ(\text{Co}^+-\text{benzene}) = 68 \pm 5$ kcal/mol¹⁵ $> D^\circ(\text{Co}^+-\text{Fe})$. In addition, previous ion-molecule bracketing studies indicate $D^\circ(\text{Co}^+-\text{Fe}) > D^\circ(\text{Co}^+-\text{CH}_3\text{CN}) > D^\circ(\text{Co}^+-\text{CH}_3) = 57 \pm 7$ kcal/mol.¹⁵ These results suggest $D^\circ(\text{Co}^+-\text{Fe}) = 62 \pm 12$ kcal/mol, in excellent agreement with the photodissociation value.

Matrix isolation of CoFe reveals that bonding is due at least partly to participation of d orbitals,³⁶ and a value of $D^\circ(\text{Co}-\text{Fe}) = 30$ kcal/mol has been calculated.³

NiFe^+ . Both Ni^+ and Fe^+ are observed as photoproducts from NiFe^+ with Ni^+ predominating. One peak at 240 nm ($\sigma = 0.20$

(32) Shim, I.; Gingerich, K. A. *J. Chem. Phys.* **1982**, *77*, 2490.

(33) Jacobson, D. B.; Freiser, B. S. *J. Am. Chem. Soc.* **1984**, *106*, 4623.

(34) Brucat, P. J.; Zheng, L.-S.; Pettiette, C. L.; Yang, S.; Smalley, R. E. *J. Chem. Phys.* **1986**, *84*, 3078.

(35) Guenzburger, D.; Baggio Saitovitch, E. M. *Phys. Rev. B* **1981**, *24*, 2368.

(36) Montano, P. A. *J. Appl. Phys.* **1978**, *49*, 1561.

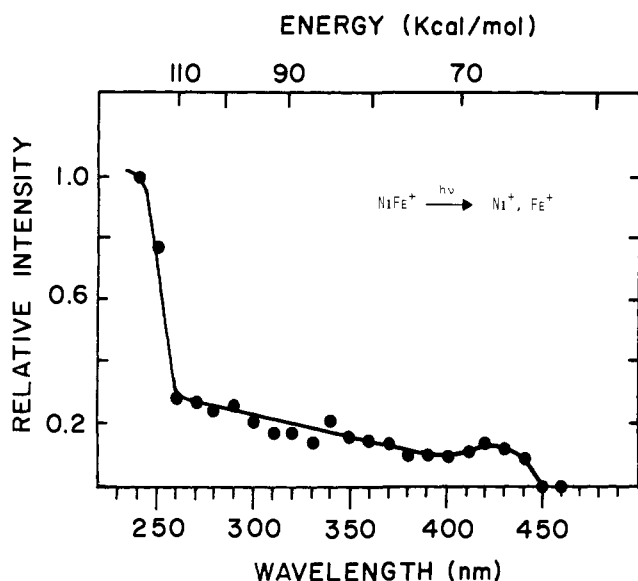


Figure 6. The photodissociation spectrum of $NiFe^+$ obtained by monitoring the appearance of Ni^+ and Fe^+ as a function of wavelength.

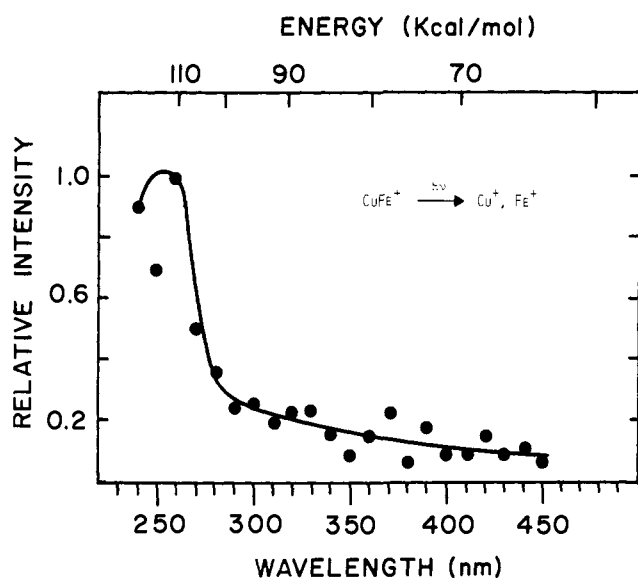


Figure 7. The photodissociation spectrum of $CuFe^+$ obtained by monitoring the appearance of Cu^+ and Fe^+ as a function of wavelength.

Å^2) is observed in the photodissociation spectrum of $NiFe^+$ (Figure 6). A cutoff at 450 nm for the appearance of Ni^+ suggests $D^\circ(Ni^+-Fe) = 64 \pm 5$ kcal/mol and $D^\circ(Fe^+-Ni) = 69 \pm 5$ kcal/mol. The threshold for appearance of Fe^+ occurs at 440 nm, suggesting $D^\circ(Fe^+-Ni) = 65 \pm 5$ kcal/mol, in reasonable agreement with the value stated above.

Benzene reacts with $NiFe^+$ to yield exclusively $NiC_6H_6^+$. Collisional activation of $NiFeC_6H_6^+$ yields predominantly $NiC_6H_6^+$ with some $NiFe^+$ also observed. These results suggest $D^\circ(Ni^+-C_6H_6) = 68 \pm 5$ kcal/mol³⁷ $>$ $D^\circ(Ni^+-Fe)$, which is consistent with the photodissociation results.

$NiFe$, observed in a rare gas matrix, is postulated to be bound almost entirely by $4s\sigma$. Theoretical calculations predict $D^\circ(Ni-Fe) = 39$ kcal/mol.^{36,38}

$CuFe^+$. Cu^+ is the major photoproduct from $CuFe^+$ although some Fe^+ is also observed. The photodissociation spectrum, shown in Figure 7, reveals one major peak at 260 nm ($\sigma = 0.40 \text{ Å}^2$) with

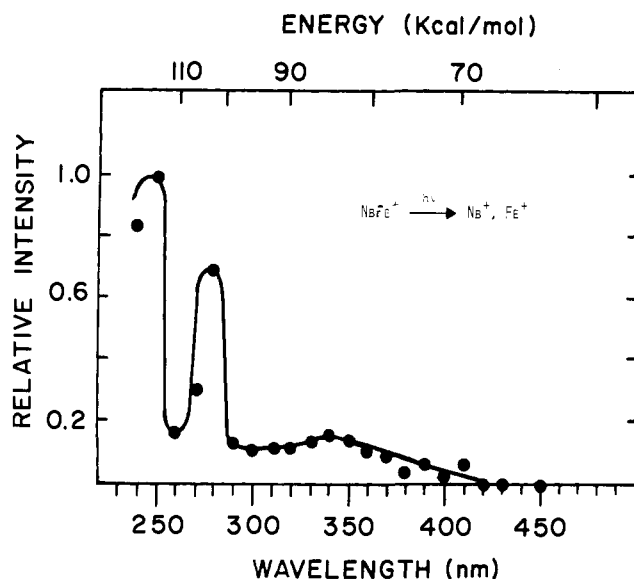
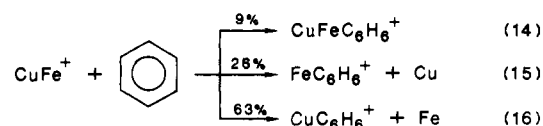


Figure 8. The photodissociation spectrum of $NbFe^+$ obtained by monitoring the appearance of Nb^+ and Fe^+ as a function of wavelength.

a dissociation threshold for Cu^+ at 540 nm, implying $D^\circ(Cu^+-Fe) = 53 \pm 7$ kcal/mol and $D^\circ(Fe^+-Cu) = 56 \pm 7$ kcal/mol. Fe^+ is observed as a photoproduct at wavelengths at least out to 450 nm, suggesting $D^\circ(Fe^+-Cu) < 64$ kcal/mol, which is consistent with the value given above.

Benzene reacts slowly with $CuFe^+$ to generate three products (reactions 14–16). Collision-induced dissociation of $CuFeC_6H_6^+$



yields predominantly $CuFe^+$ with some $CuC_6H_6^+$ also observed. The appearance of $CuFe^+$ from collisional activation of $CuFeC_6H_6^+$ suggests $D^\circ(Fe^+-Cu) >$ $D^\circ(Fe^+-C_6H_6) = 55 \pm 5$ kcal/mol, which implies $D^\circ(Cu^+-Fe) >$ 52 ± 5 kcal/mol.²⁷ This lower limit for $D^\circ(Cu^+-Fe)$ is consistent with the photodissociation results. CID of $CuFeC_6H_6^+$ and observation of reaction 16 (believed to be 1–3 kcal/mol endothermic) suggest $D^\circ(Cu^+-Fe)$ is only slightly greater than $D^\circ(Cu^+-benzene)$, implying $D^\circ(Cu^+-C_6H_6) = 50 \pm 9$ kcal/mol. Cu^+ is unreactive with cyclohexane and cyclohexene, yielding no additional information about $D^\circ(Cu^+-C_6H_6)$.

Matrix isolation suggests a strong bond between Cu and Fe.⁴¹ $D^\circ(Cu-Fe) = 30$ kcal/mol has been predicted.³

$NbFe^+$. $NbFe^+$ photodissociates to give primarily Nb^+ with some Fe^+ also observed. Two peaks are observed in the photodissociation spectrum of $NbFe^+$ (Figure 8) at 250 ($\sigma = 0.55 \text{ Å}^2$) and 280 nm. The onset for photoappearance of Nb^+ occurs at 420 nm, suggesting $D^\circ(Nb^+-Fe) = 68 \pm 5$ kcal/mol and $D^\circ(Fe^+-Nb) = 91 \pm 5$ kcal/mol. Observation of Fe^+ at wavelengths at least out to 310 nm requires $D^\circ(Fe^+-Nb) < 92$ kcal/mol.

$NbFe^+$ does not react with benzene, implying $D^\circ(Nb^+-Fe) >$ $D^\circ(Nb^+-C_6H_6)$ and $D^\circ(Fe^+-Nb) >$ $D^\circ(Fe^+-C_6H_6)$. CID of $NbFeC_6H_6^+$, from cyclohexene and $NbFe^+$, yields $NbFe^+$ exclusively, verifying the limits stated above. Nb^+ will dehydrogenate hexane to benzene, requiring $D^\circ(Nb^+-C_6H_6) \geq 60$ kcal/mol.³⁹ Taken in total, these results indicate $D^\circ(Nb^+-Fe) > 60$ kcal/mol.

$NbFe$ has not been observed experimentally, but $D^\circ(Nb-Fe) = 59$ kcal/mol has been calculated.¹

$TaFe^+$. $TaFe^+$ photodissociates as expected to both Ta^+ and Fe^+ , in roughly equal intensity. Figure 9, the photodissociation spectrum of $TaFe^+$, reveals one peak at 240 nm with a cross section $\sigma(240 \text{ nm}) = 0.20 \text{ Å}^2$. The photoappearance threshold of Ta^+

(37) Jacobson, D. B.; Freiser, B. S., unpublished results.

(38) Shim, I. *Theor. Chim. Acta* **1981**, *59*, 413.

(39) Buckner, S.; MacMahon, T.; Freiser, B. S. *Organometallics*, in preparation.

(40) Lin, S.-S.; Kant, A. J. *J. Phys. Chem.* **1969**, *73*, 2450.

(41) Rohlfiing, E. A.; Cox, D. M.; Kaldor, A.; Johnson, K. H. *J. Chem. Phys.* **1984**, *81*, 3846.

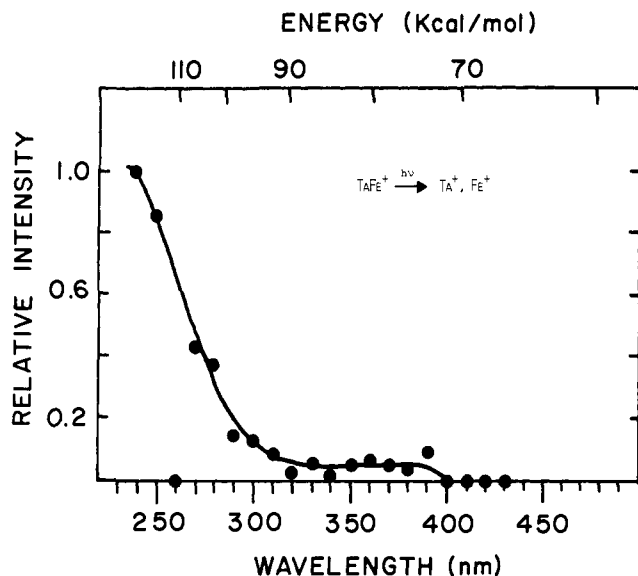


Figure 9. The photodissociation spectrum of TaFe^+ obtained by monitoring the appearance of Ta^+ and Fe^+ as a function of wavelength.

occurs at 400 nm, implying $D^\circ(\text{Ta}^+-\text{Fe}) = 72 \pm 5$ kcal/mol and $D^\circ(\text{Fe}^+-\text{Ta}) = 72 \pm 5$ kcal/mol. The threshold for formation of Fe^+ also occurs at 400 nm, verifying $D^\circ(\text{Fe}^+-\text{Ta})$ given above.

Collision-induced dissociation of $\text{TaFeC}_6\text{H}_6^+$, formed by reacting TaFe^+ with cyclohexene, yields TaFe^+ exclusively, implying $D^\circ(\text{Ta}^+-\text{Fe}) > D^\circ(\text{Ta}^+-\text{C}_6\text{H}_6)$ and $D^\circ(\text{Fe}^+-\text{Ta}) > D^\circ(\text{Fe}^+-\text{C}_6\text{H}_6) = 55 \pm 5$ kcal/mol.¹⁵ Ta^+ will dehydrogenate cyclohexane to benzene, requiring that $D^\circ(\text{Ta}^+-\text{C}_6\text{H}_6)$ exceed 60 kcal/mol.⁴⁰ These ion-molecule reactions give a lower limit $D^\circ(\text{Ta}^+-\text{Fe}) > 60$ kcal/mol. Finally, taken together these results also indicate 72 ± 5 kcal/mol $> D^\circ(\text{Ta}^+-\text{C}_6\text{H}_6) > 60$ kcal/mol.

A calculated $D^\circ(\text{Ta}-\text{Fe}) = 60$ kcal/mol is predicted,¹ but no experimental data have been reported.

MFe⁺ Bonding. Heteronuclear metal cluster ions photodissociate readily in the ultraviolet and visible spectral regions and appear to provide a wealth of experimental information. Bond energies determined by photodissociation show good agreement with values obtained by ion-molecule reactions. Evidently, there are many low-lying electronic states that allow thresholds to be controlled by thermodynamic factors. Absorption spectra for a variety of neutral homonuclear clusters have been obtained, and they also reveal extensive absorption in the ultraviolet and visible spectral regions.^{9c,31}

Few if any experimental bond energies are available for MFe neutral clusters, but several theoretical values have been calculated. With the exception of ScFe^+ , the bond energies for the cluster ions greatly exceed the bond energies for the cluster neutrals. The positive charge on the cluster ion may reduce the internuclear distance of the two metals enough to allow d-d electron bonding to become more prevalent in the ions than in the neutral clusters. Surprisingly, the calculated bond energies of MFe are completely unrelated to the experimental bond energies of MFe^+ .

The ionization potentials of the neutral clusters can be calculated from $D^\circ(\text{M}-\text{Fe})$ and $D^\circ(\text{M}^+-\text{Fe})$ by eq 17 (M is a transition

metal). $D^\circ(\text{M}-\text{Fe})$ has been calculated for many clusters, and

$$\text{IP}(\text{MFe}) = D^\circ(\text{M}-\text{Fe}) + \text{IP}(\text{M}) - D^\circ(\text{M}^+-\text{Fe}) \quad (17)$$

$D^\circ(\text{M}^+-\text{Fe})$ can be obtained by observing photoappearance thresholds. The uncertainties in the calculated bond energy values for the neutrals give rise to at least ± 0.5 eV for $\text{IP}(\text{MFe})$. Table I summarizes the ionization potentials, calculated with eq 17, for the clusters examined in this study. The ionization potential for Fe_2 calculated in this manner ($\text{IP}(\text{Fe}_2) = 6.0$ eV) shows excellent agreement with an early determination of 5.9 eV⁴⁰ and good agreement with the most recently determined experimental value $\text{IP}(\text{Fe}_2) = 6.3 \pm 0.01$ eV.⁴¹ The ionization potentials for these ions are found to be in the range of 5.4–7.0 eV and are consistently lower than the ionization potentials for the metal atoms. There is no correlation between $\text{IP}(\text{MFe})$ and $\text{IP}(\text{M})$. For comparison, the ionization potentials of homo- and heteronuclear alkali dimers are in the 3.7–5.0 eV range.⁴² Kaldor et al. have observed that the ionization potentials for iron clusters depend on the cluster size, with a range of 5.0–8.0 eV.⁴³

The bonding in MFe^+ is difficult to ascertain and awaits further detailed theoretical consideration. It seems reasonable to postulate that d orbital contribution to the bonding in MFe^+ is greatest when M is an early transition metal (i.e., $\text{M} = \text{Sc}$ through Fe). The d orbitals of early transition metals, which are larger in size than the d orbitals of later transition metals, are partially empty and can readily accept electron density. For clusters MFe^+ where M is a late transition metal (i.e., $\text{M} = \text{Co}$ through Cu), even if d orbital overlap occurs, there will be a significant number of electrons in antibonding orbitals. This factor would reduce the stabilization of MFe^+ due to d electron contribution and may imply that bonding in MFe^+ for $\text{M} = \text{Co}$ through Cu may primarily be due to 4s electron overlap.

The photodissociation of transition metal cluster ions provides a convenient route for probing the bonding nature of small metal clusters. Generation and photodissociation of cluster ions is a difficult but not impossible task and should permit examination of not only dimers but also larger clusters.

Acknowledgment is made to the Division of Chemical Sciences in the Office of Basic Energy Sciences in the United States Department of Energy (DE-AC02-80ER10689) for supporting the transition metal ion research and to the National Science Foundation (CHE-8310039) for continued support of the Fourier transform mass spectrometry instrumentation. The authors thank D. B. Jacobson for helpful discussions. R. L. H. gratefully acknowledges the W. R. Grace Co. for providing fellowship support.

Registry No. ScFe^+ , 107474-37-3; TiFe^+ , 107474-38-4; VFe^+ , 98330-71-3; CrFe^+ , 107474-39-5; Fe_2^+ , 61674-68-8; CoFe^+ , 91295-14-6; NiFe^+ , 71232-34-3; CuFe^+ , 107474-40-8; NbFe^+ , 107474-41-9; TaFe^+ , 107474-42-0; Fe^+ , 14067-02-8; Sc^+ , 14336-93-7; Ti^+ , 14067-04-0; Cr^+ , 14067-03-9; Co^+ , 16610-75-6; Ni^+ , 14903-34-5; Cu^+ , 17493-86-6; Nb^+ , 18587-63-8; Ta^+ , 20561-66-4; C_6H_6 , 71-43-2; $\text{Sc}(\text{C}_6\text{H}_6)^+$, 107494-94-0; $\text{Ti}(\text{C}_6\text{H}_6)^+$, 107494-95-1; $\text{Cr}(\text{C}_6\text{H}_6)^+$, 107494-96-2; $\text{Fe}(\text{C}_6\text{H}_6)^+$, 102307-51-7; $\text{Co}(\text{C}_6\text{H}_6)^+$, 102307-50-6; $\text{Ni}(\text{C}_6\text{H}_6)^+$, 107494-97-3; $\text{Cu}(\text{C}_6\text{H}_6)^+$, 107494-98-4; cyclohexene, 110-83-8.

(42) Kappes, M. M.; Schar, M.; Schumacher, E. *J. Phys. Chem.* **1985**, *89*, 1499.

(43) Kaldor, A.; Rohlfing, E.; Cox, D. M. *Laser Chem.* **1983**, *2*, 185.